ARTICLES

Mechanism of Stationary Bulk CO Oxidation on Pt(111) Electrodes†

E. A. Batista, T. Iwasita,* and W. Vielstich*

Instituto de Química de São Carlos, Universidade de São Paulo, Cx. P. 780, CEP 13560-970, Brazil

Received: December 25, 2003; In Final Form: May 24, 2004

Carbon monoxide oxidation at platinum electrodes in acid solutions presents a characteristic behavior depending on the presence or not of dissolved CO in the bulk of the solution. In the present paper, bulk CO electrooxidation is studied on a Pt(111) electrode. A change of the (2×2)-3CO overlayer, formed by admitting CO at 0.05 V, into a $(\sqrt{19} \times \sqrt{19})$-13CO structure was observed at around 0.4 V. These changes were monitored by in situ Fourier transform IR spectroscopy through the bands for on-top, 2-fold, and 3-fold bonded CO. If the solution is saturated with CO, oxidation of the CO adlayer formed at 0.05 V begins at ca. 0.4 V and presents a "quasistationary" behavior. This process involves weakly bonded CO. The presence of such species is rationalized in terms of the steep decrease of the desorption energy at high degrees of coverage, reported for CO adlayers on Pt(111) in UHV. When CO is adsorbed at *high potentials* (above 0.6 V), segregated adlayers of CO and H-bonded H_2O are formed. The H-bonded H_2O clusters represent a barrier for water activation, and thus, the oxidation of CO is inhibited. The influence of the CO partial pressure in solution on the reaction rate is also studied. These results allow inferring that bulk CO oxidation follows a Langmuir−Hinshelwood mechanism.

1. Introduction

The oxidation of carbon monoxide is one of the issues of major interest in electrocatalysis.[1,2] Carbon monoxide is formed as an intermediate during the oxidation of small organic molecules on Pt-based catalysts. Small (ppm) amounts of CO, present as a contamination in the reformer gas used to feed H_2 fuel cells, act as a catalyst poison. This fact has motivated an intensive search for CO-tolerant anodes.[3] Moreover, in former times, CO itself was investigated as an active substance for fuel cells.[4] A wealth of data covering studies in ultrahigh vacuum[5] and in electrochemical systems[6] is now available. Despite its simplicity, CO presents quite a complex behavior in electrochemical cells and its understanding is a key point in electrocatalysis.

At the metal−electrolyte interface, the rate of CO oxidation reaction depends on several experimental parameters such as surface structure, adsorption potential, and degree of coverage. Additionally the onset potential for oxidation depends on whether CO is or not present in the bulk of the solution.

The oxidative stripping of adsorbed carbon monoxide (CO_{ad}) presents a marked dependence on the admission potential, as has been reported several times.[7] The same is valid for the oxidation process in the presence of CO in the bulk of the solution (CO_{bulk}) at polycrystalline Pt and at single-crystal Pt(111).[8,9] Thus, a cyclic voltammogram (CV) for adsorbed CO at 0.05 V vs RHE on Pt(111), obtained in a *CO-free solution*, exhibits a sharp, well-defined, peak at 0.75 V. The onset potential for CO oxidation is at ca. 0.42 V, and a small prepeak is observed at ca. 0.62 V. This prepeak is absent for adsorption potentials above 0.3 V.

A different oxidation behavior is observed in the presence of CO in the bulk *of the solution*. In this case, besides a sharp oxidation peak at 0.85 V, a well-defined peak centered at ca. 0.70 V is observed if CO is admitted in the cell at a potential near 0.05 V. However, if the upper potential of the scan is as high as 1.2 V, the latter peak occurs only during the *first* scan. The following scans do not show up the large current in the region of the prepeak, and in addition, the maximum rate of oxidation for the main peak is shifted to higher potentials. On the other hand, using an admission potential above ca. 0.4 V, the first cycle is already the same as the second and subsequent cycles.

The behavior described above indicates that the reactivity of CO toward oxidation possibly depends on structural changes in the CO overlayer, which, in turn, depends on the admission potential. In this respect, it is interesting to recall some literature results on CO adsorption at Pt(111), using STM and in situ Fourier transfrom (FT)IR,[10,11] which show that the CO ad-layer structure exhibits a pronounced dependence on the applied potential. Figure 1 shows STM images and FTIR spectra from ref 10, obtained in the presence of dissolved CO in 0.1 M $HClO_4$. At potentials below 0.4 V, a (2×2)-3CO close-packed structure is observed (Figure 1a), for which an infrared spectrum, Figure 1c, exhibits on-top CO (2066 cm^{-1}) and 3-fold bonded CO (1773 cm^{-1}). This structure implies a coverage degree of $\theta_{CO} = 0.75$. At potentials above 0.4 V, a $(\sqrt{19} \times \sqrt{19})$-13CO structure is observed (Figure 1b), which corresponds to a coverage degree of $\theta_{CO} = 0.68$. The corresponding spectrum exhibits bands for on-top CO and bridge-bonded CO (1850 cm^{-1}). It has been shown later that the potential at which the

† Part of the special issue "Gerhard Ertl Festschrift".

* To whom correspondence may be addressed. E-mail: Iwasita@iqsc.usp.br (T.I.); Vielstich@iqsc.usp.br (W.V.).

10.1021/jp038016+ CCC: $27.50 © 2004 American Chemical Society
Published on Web 08/06/2004

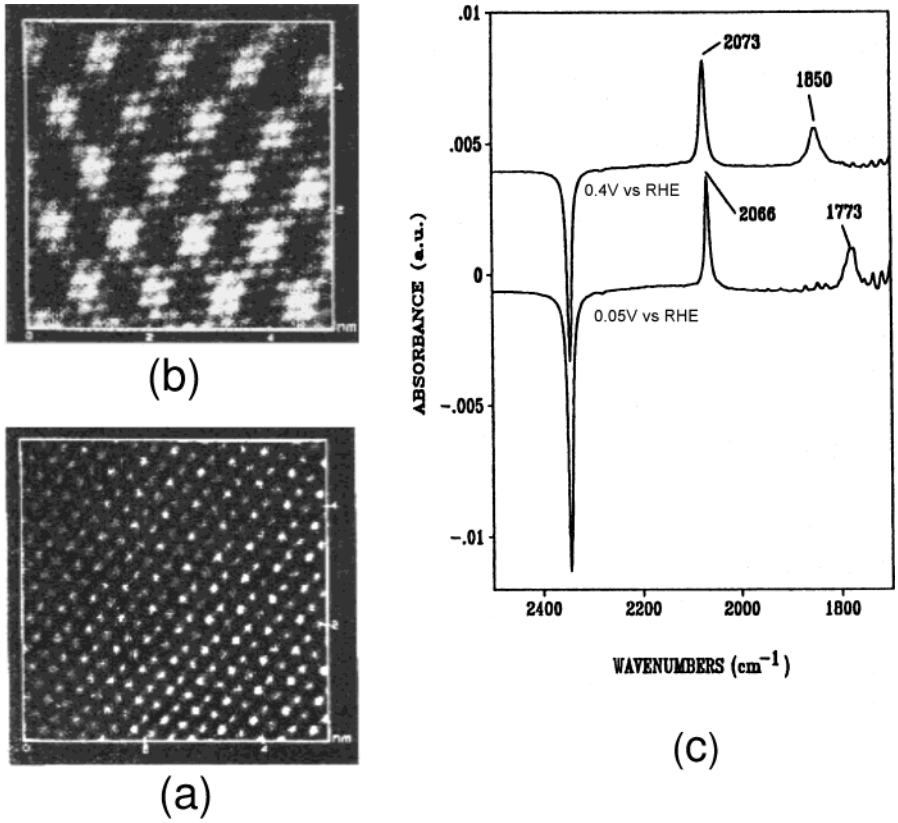

Figure 1. STM and FTIRS of carbon monoxide adsorbed at Pt(111) in the presence of dissolved CO in 0.1 M $HClO_4$. (a) (2×2)-3CO structure obtained at 0.05 V vs RHE and (b) $(\sqrt{19} \times \sqrt{19})23.4°$-13CO structure obtained at 0.4 V vs RHE. (c) In situ FTIR spectra at 0.05 and 0.40 V vs RHE as indicated in the spectra. See band assignment in the text. From ref 10, published with permission of the American Institute of Physics.

phase transition occurs depends on the width of the (111) terraces and on the presence of surface defects.[12] X-ray diffraction studies on the system also detected the ordered (2×2)-3CO structure at low potentials.[13] However, no change to the $(\sqrt{19} \times \sqrt{19})$-13CO or any other ordered structure was detected by X-ray diffraction, leading to the conclusion that such structure can exist only in small patches and does not show a long range order.[13]

The present work was undertaken with the aim of gaining new knowledge related to the oxidation process in CO saturated solution, using Pt(111), for which STM and IR data exist. The supporting electrolyte was 0.1M $HClO_4$. In addition to the electrochemical methods, in situ FTIR was used for monitoring the surface processes at a molecular level.

2. Experimental Section

All solutions were prepared with MilliQ water and 0.1 M $HClO_4$ (Merck, *pro analyze*) as a supporting electrolyte. The gases used were CO (99.5%) and N_2 (5.0) from White Martins.

The working electrode was a Pt(111) disk (Ma-Teck) having a surface area of 0.78 cm^2. Before each experiment, the electrode was annealed in a H_2 flame and cooled in a H_2/Ar stream. Then the electrode was transferred to the cell, protected by a droplet of water in equilibrium with the cooling gases. Immediately after contacting the solution, the electrode was kept under a controlled potential of 0.05 V. The quality of the surface was checked by cyclic voltammetry in the base electrolyte solution, using a meniscus configuration as usual.

The counter electrode was a Pt sheet forming a flat ring of 4.7 cm^2. Throughout the experiments, the reference electrode was a hydrogen electrode in the same solution (RHE).

IR spectra were measured using a spectrophotometer Nicolet, model Nexus 670, provided with a MCT detector. The electrochemical cell[14] was externally placed on the upper part of the IR-sample chamber, with the electrode in a horizontal position. A two-mirror attachment was used to focus the IR beam on the electrode surface and on the detector.

3. Results and Discussion

3.1. Cyclic Voltammetry and Potential Step Experiments. The voltammogram shown in Figure 2a was obtained in a CO-saturated solution after CO admission at 0.05 V. A high oxidation current is observed at potentials below 0.6 V during the first cycle. If the positive end of the voltammogram is 1.2 V, the current in the region below 0.6 V decreases to very low values during the second and subsequent scans. Figure 2b shows a voltammogram during the stripping of a CO monolayer (no CO in the solution), for comparison.

If the positive end of the voltammogram is below 0.6 V, only a slight decrease in current is observed during the subsequent scans, as shown in Figure 3. Inhibitory effects on the CO bulk oxidation are mainly related to some process occurring during the cycling at potentials above 0.6 V. It was observed that, as the positive limit of the CV is extended, the oxidation current in the low potential region gradually diminishes during the second and subsequent scans. Finally, for a positive limit of 1.2 V, the processes at low potentials are inhibited already in the second scan as shown in Figure 2a.

Further details on the behavior described above were obtained through the potential step experiments shown in Figure 4. There, the current is shown for a sequence of applied potentials as indicated. The admission potential for this experiment was 0.05 V. At first, the potential was stepped to 0.6 V and the current

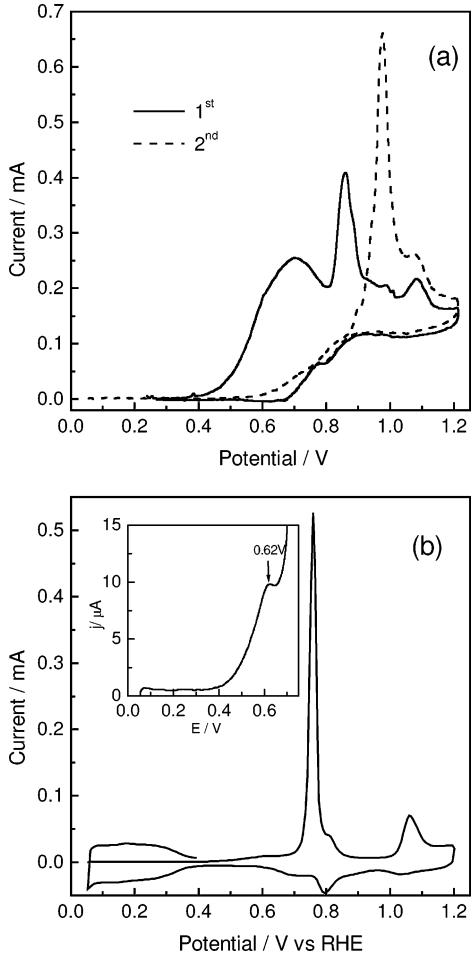

Figure 2. (a) First and second cycles from potential sweeps between 0.05 V and 1.2 V for a Pt(111) electrode in CO saturated 0.1 M $HClO_4$ solution; $\upsilon = 50$ mV/s. CO was admitted in the cell at 0.05 V. (b) Cyclic voltammogram for a Pt(111) electrode with an adsorbed CO layer in a 0.1 M $HClO_4$ solution. CO was adsorbed at 0.05 V; afterward CO was eliminated from the solution by bubbling Ar during 15 min.

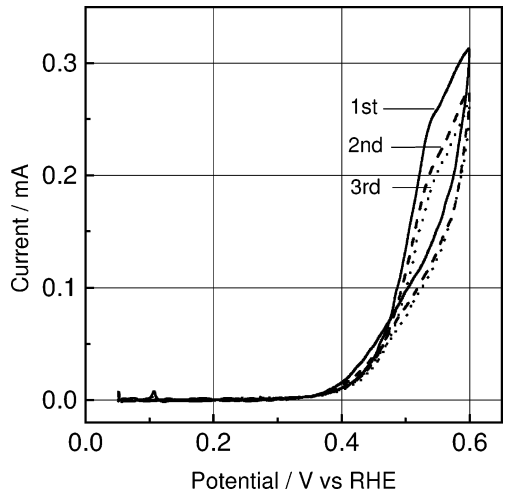

Figure 3. Repetitive cyclic voltammogramms (1−3) between 0.05 and 0.6 V for a Pt(111) electrode in CO saturated 0.1 M $HClO_4$ solution; $\upsilon = 50$ mV/s. CO was admitted in the cell at 0.05 V.

was monitored during ca. 5 min. Subsequently, the potential was changed to 1.2 V and then back to 0.6 V. A marked loss in activity is observed, which is not recovered by a step to 0.05 V (a longer stay at 0.05 V does not change this result). The electrode only recovers the original activity after the sequence 0.6 V → 1.2 V → 0.05 V → 0.6 V. At the potential of 1.2 V,

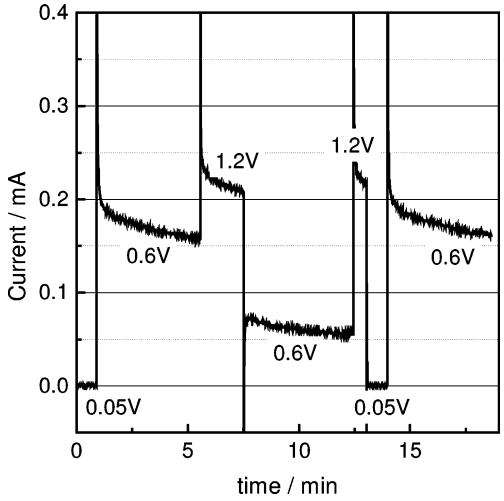

Figure 4. Current−time responses for bulk CO oxidation at Pt(111) in 0.1M $HClO_4$ solutions. A series of potential steps were successively applied as indicated in the figure.

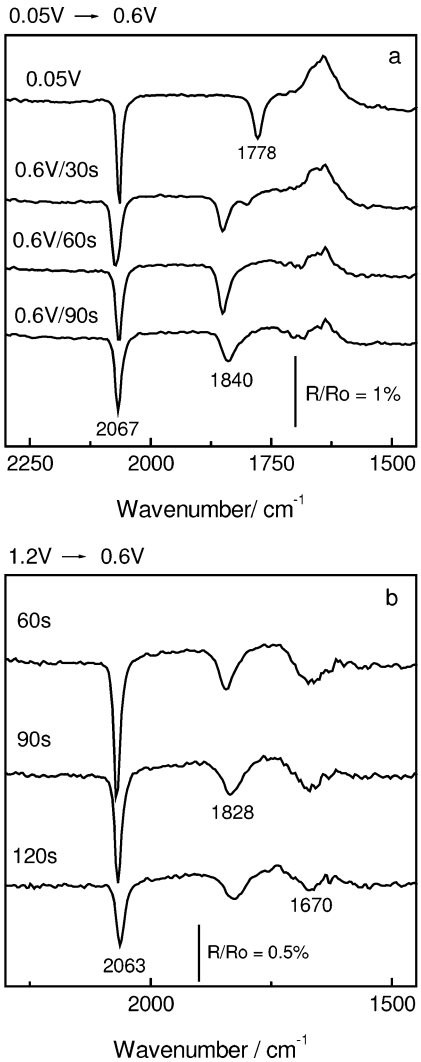

Figure 5. In situ FTIR spectra for a Pt(111) electrode in CO-saturated 0.1 M $HClO_4$: (a) Spectra measured at 0.05 V and after a step 0.05 → 0.6 V (time dependence as indicated). (b) Spectra at 0.6 V after a potential step 1.2 → 0.6 V (time dependence as indicated). For both sets a and b, the reference spectrum was measured at 1.2 V.

the rate of CO oxidation is high and the electrode surface is practically free of adsorbed CO. On the contrary, at 0.05 V and 0.6 V as well, the surface becomes covered by CO. Thus, we

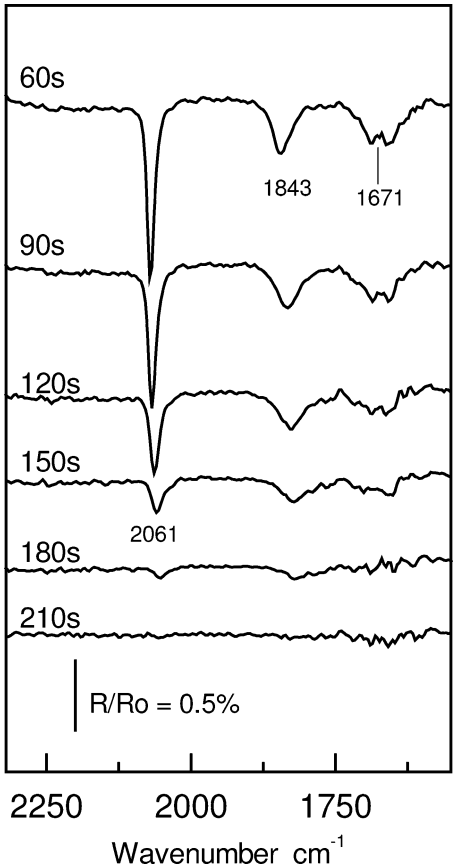

Figure 6. In situ FTIR spectra for a Pt(111) electrode in CO-saturated 0.1 M $HClO_4$ solution showing the disappearance of CO bands with time, due to the depletion of bulk CO in the thin layer. Sequence of potential applied was 1.2−0.6 V as in Figure 5b but taking as a reference the spectrum measured after 240 s. After this time, all bulk CO has been oxidized and also the surface is free from CO_{ad}.

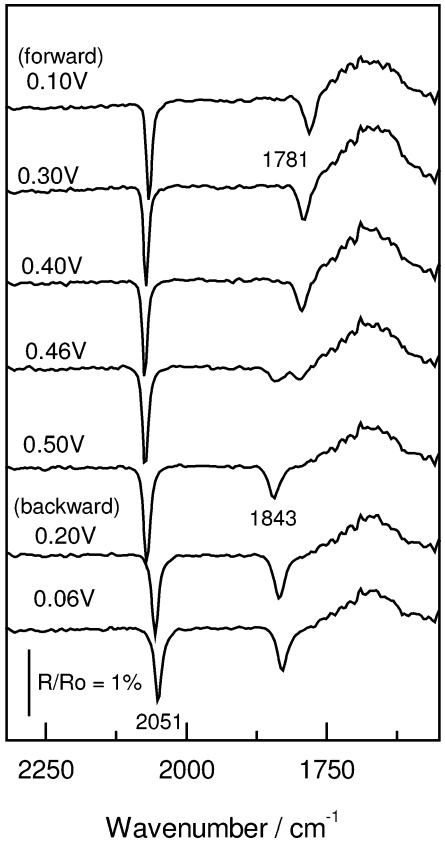

Figure 7. Potential-dependent in situ FTIR spectra at a Pt(111) surface in CO-saturated 0.1 M $HClO_4$ solution. The potential was applied in 0.02 V steps from 0.1 V to 0.5 V and back to 0.06 V as indicated. The reference spectrum was taken after finishing the sequence, at 0.95 V. Admission potential was 0.05 V.

conclude that the catalytic activity is likely related to the kind of CO overlayer formed at the respective potential, the one at 0.05 V allowing for a higher activity at low potentials. In addition, the surface processes involved seem to be irreversible, at least in the time scale of the steps in the above experiments (some minutes). This interpretation of the above results requires the support of spectroscopic data as presented in the next section.

3.2. In situ FTIR Results. Infrared spectra were measured after applying potential steps from 0.05 V and from 1.2 V to the final potential of 0.6 V. The results are shown in parts a and b of Figure 5. To obtain absolute bands for CO, both sets of spectra were calculated using a spectrum obtained at 1.2 V, i.e., a potential where adsorbed CO is completely oxidized. The spectra in Figure 5a, corresponding to the potential step 0.05 → 0.6 V, show the change of surface structure, (2×2)-3CO→ $(\sqrt{19} \times \sqrt{19})$-13CO, reflected in the transformation of 3-fold bonded CO (1780 cm^{-1}) into bridge-bonded CO (1840 cm^{-1}).[10]

The series of spectra 5b show up as a band for the bending mode of H_2O at a relatively high frequency of 1670 cm^{-1}. (For liquid water in the electrochemical environment, the bending mode is usually observed at 1642 cm^{-1}.)[14] This band is less defined in Figure 5a, probably due to the positive-going feature, at 1642 cm^{-1}, which is due to uncompensated liquid water in the thin layer of solution between the electrode and the IR window.[15] The band at 1670 cm^{-1} is negative, indicating that the responsible species is formed at 0.6 V and was not present at 1.2 V (reference potential). The high value of the bending mode can be due to strong lateral interactions of the water molecules with other components of the adlayer (CO) and/or to the formation of hydrogen bonds since, according to ref 15, H-bond formation shifts the bending mode toward higher frequencies. It must be noted that the band intensity for adsorbed CO decreases with time. This effect, which is more pronounced in set b of spectra, is due to the consumption of CO in the thin layer between the electrode and the IR window. The bulk concentration of CO in a saturated solution is relatively low (ca. 10^{-3} M),[16] and its depletion, in a thin layer of some μm thickness, can take place within a few minutes.[17] Making use of this fact, we have monitored the change with time of spectra taken under the conditions of Figure 5b, i.e., after a potential step from 1.2 to 0.6 V. In this case, a spectrum taken after 240 s showed up no CO bands and could, therefore, be used as a reference. The results are shown in Figure 6. One can observe that the intensity of the water feature at 1673 cm^{-1} encompasses the loss of intensity of the CO bands. It is, thus, obvious that the 1670 cm^{-1} band of water must be associated with the kind of CO adlayer formed at 0.6V.

Monitoring of the Adlayer Changes with Potential. A series of spectra taken by applying sequential potential steps (0.02 V) from 0.05 V (admission potential) to 0.5 V and back is given in Figure 7. The adlayer transition $(2 \times 2) \rightarrow (\sqrt{19} \times \sqrt{19})$ (characterized by the change of 3-fold to 2-fold bonded CO) is observed in the spectrum at 0.46 V. According to ref 12, the potential for the phase transition depends on the size of the (111) terraces and is shifted to values between 0.5 V and 0.6 V for larger (111) terraces. Note that in the series of spectra of Figure 7 the H-bonded water feature at 1670 cm^{-1} is absent. This is an indication that this kind of water is not formed during the phase transition. After measuring the spectrum at 0.5 V, the direction of the potential step was reversed. The lowering of

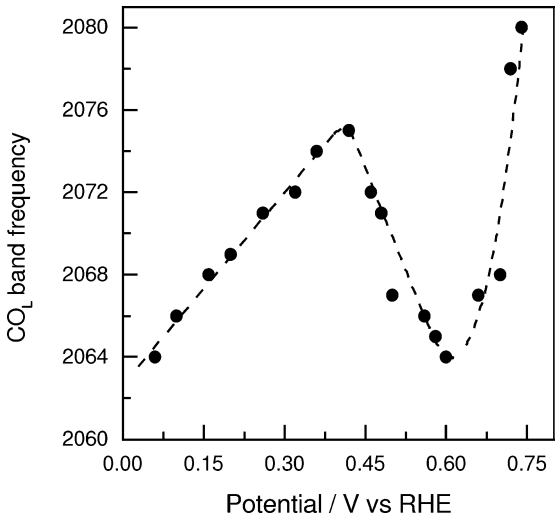

Figure 8. Potential dependence of the band center frequency for on-top CO as measured from a series of spectra in CO saturated 0.1 M $HClO_4$ solution at different increasing potentials measured under the same conditions as in Figure 7.

the intensity of linear bonded CO in the spectra measured at 0.20 V and 0.06 V is a consequence of the consumption of bulk CO in the thin layer of solution between the electrode and the IR window. The (2×2) structure is not recovered within the time scale of this experiment (ca. 5 min). But, if the electrode is pulled back in order to saturate the solution in the thin layer, the (2×2) structure is formed again. This is in agreement with results of X-ray scattering at Pt(111) in CO saturated solutions obtained under a constant supply of a CO overpressure.[13] The results show that the (2×2) structure is recovered at 0.2 V, during a potential sweep from 0.7 V in the negative direction.

In Figure 8 are plotted the band center frequencies for on-top CO taken from a series of spectra obtained at increasing potentials. The frequency increases initially presenting a Stark shift of 31 cm^{-1}/V. As the phase transition occurs, at 0.46 V, a sudden fall of frequency is observed and after a minimum value attained at 0.6 V, the frequency increases again at a much higher rate of ca. 190 cm^{-1}/V. Similar results were observed by Yoshimi and Ito for CO admitted with the beginning of the phase transition. In ref 11, in the presence of 0.1M H_2SO_4, the falling of frequency was observed at 0.4 V. But we have checked that the potential difference is related to the different supporting electrolyte.

3.3. Approaching Some Ideas on the Electrooxidation Process. As explained in the Introduction, the phase transition (2×2)-3CO$\rightarrow$$(\sqrt{19} \times \sqrt{19})$-13CO causes a change in θ_{CO} from 0.75 to 0.68. This "opening" of the CO surface structure allows the entrance of water in the adlayer and permits the oxidation of CO to CO_2.[11] However, it was shown in Figure 3 that the onset potential for CO oxidation is about 0.35 V. This early oxidation process can be caused by the activation of water present at some defects of the CO overlayer. Recall that the phase transition using Pt(111) surfaces presenting large terraces can be shifted to 0.5−0.6 V.[12]

Taking into account that the overlayer transition occurs at ca. 0.46 V (Figure 7), the sustained catalytic activity observed in Figure 3 occurs mainly in the presence of a $(\sqrt{19} \times \sqrt{19})$ overlayer. It should be noted that, according to Lucas et al.,[13] oxidation of a small fraction (15%) of the adlayer strongly affects the (2×2)-3CO phase.

As shown before (Figure 5b), if a potential step is applied from 1.2 to 0.6 V in the presence of a saturated CO solution, a H_2O/CO overlayer is formed. Since at 1.2 V the surface is free from adsorbed CO, the potential of 0.6 V can be considered as an "admission potential". On a clean surface (formed by stepping the potential from 1.2 to 0.6 V) CO and H_2O are coadsorbed in the form of juxtaposed islands.[18] Recall that adsorbed water exhibits in this case a very high bending frequency (1670 cm^{-1}), indicating the presence of H-bonds, i.e., water clusters are formed. Kitamura and Ito observed in H_2SO_4 a water band at 1666 cm^{-1} for an admission potential of 0.4 V, which they attributed to an ice structure formed on top of the CO adlayer.[11] According to these authors, this water layer was responsible for a lowering of the catalytic activity toward CO oxidation. It seems to us, that the band at 1670 cm^{-1} corresponds to the same water species as that observed in ref 11. However, under the conditions of the experiment in Figure 6, at 0.6 V and with CO being not only adsorbed but also oxidized, it seems unlikely to form a CO adlayer exhibiting a long-range order with an ice water layer on top. Such a structure could only be possible in the form of small surface patches. But the fact that the kind of water involved appears only when water molecules have access to the surface at high potentials (e.g., when the CO adlayer is formed at 0.6 V) could be an indication that water clusters are directly inserted between the CO islands. The CO−H_2O repulsive interaction[18] results in H-bonded water clusters and a weakening of the H_2O−metal interaction. This suggests that the activation of H_2O for CO oxidation is hindered. Summarizing, when the potential is stepped from 1.2 V to 0.6 V (Figure 4), the current for CO oxidation is low because of the unfavorable conditions to dissociate a single H_2O molecule out of the H-bonded cluster.

The inhibitory effect is not present when the CO adlayer is formed at 0.05 V, probably because at this potential CO adsorbs, displacing a layer of adsorbed hydrogen. The direct interaction of water molecules with the surface is necessary for the formation of a H_2O inhibiting structure. This condition explains why the blocking structure is formed during the negative going sweep of a voltammogram: the CO islands are formed on a surface initially covered with water, giving rise to the possibility of forming the H_2O clusters. On the other hand, cycling the potential between 0.05 V and 0.6 V in the presence of a CO adlayer formed at 0.05 V causes only a slight lowering in the activity for CO oxidation since, under such conditions, a high degree of CO coverage keeps the surface "protected" against the formation of H_2O clusters.

Electro-oxidation of CO in the Prepeak Region. As the stripping voltammogram in Figure 2b shows, a small peak current is observed in the potential region around 0.60V. This so-called pre-peak is only observed in the absence of bulk CO if the CO adlayer is saturated. The charge under this peak is well below the charge under the main stripping peak at 0.75 V. Obviously, the corresponding processes involve energetically different species of CO. Since the prepeak is only observed under conditions of high degrees of coverage, it is possible that the energy of desorption for these species is being lowered due to repulsion between neighboring CO molecules. Under UHV conditions, it was observed that the energy of desorption of CO decreases steeply as the degree of coverage reaches saturation.[19] Thus, the CO species being oxidized under the prepeak should be considered as weakly bonded to the surface. As these species are oxidized, the coverage diminishes slightly but the energy of desorption increases steeply and further oxidation of the CO adlayer requires the application of a higher potential (main oxidation peak at 0.75 V in Figure 2b).

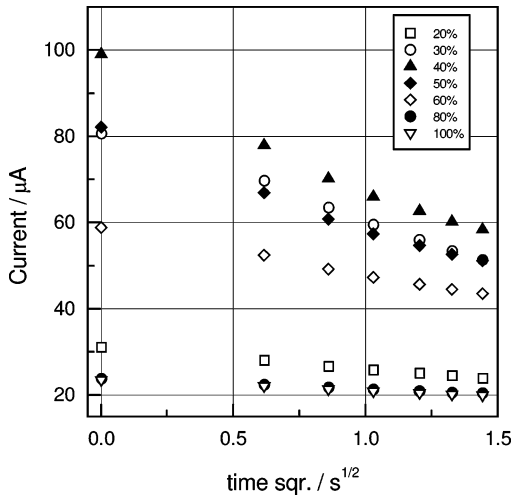

Figure 9. Dependence of the current at 0.5 V on the square root of time, for bulk CO oxidation at Pt(111) in 0.1M $HClO_4$ solution. CO concentration in the gas mixture (CO/N_2) used to saturate the solution are as indicated in the inset.

In the presence of bulk CO, on the other hand, the coverage degree can be kept high and a sustained oxidation of weakly bonded CO at low potentials causes the current observed in the voltammogram of Figures 2a and 3. The process under this experimental condition is discussed in the next section.

The Influence of the CO Partial Pressure. It is generally accepted that the stripping reaction, i.e., the oxidation of a monolayer of adsorbed CO, proceeds through a Langmuir−Hinshelwood mechanism (L−H) between adsorbed CO and adsorbed H_2O or adsorbed OH.[20] Denoting the adsorbed species with (ad)

$$CO_{ad} + OH_{ad} \rightarrow CO_2 + H^+ + e^-$$

The understanding of the oxidation reaction in the CO-saturated solution requires further knowledge on the current dependence on the bulk CO concentration. From these data, we expect to learn more about the mechanism of the reaction. For this purpose, the CO concentration in the bulk of the solution was systematically changed and the current−time responses were measured after the application of a potential step to 0.5 V. The procedure was as follows. First, the Pt(111) electrode was immersed in the 0.1 M $HClO_4$ solution and a potential of 0.05 V was applied. Pure CO was bubbled during 5 min to reach saturation of the surface. Then the gas composition was changed by dilution with N_2, and the mixture was bubbled during 20 min in order to change the CO concentration in the bulk of the solution. After this, the gas bubbling was stopped. The electrode was positioned on the surface in a meniscus configuration, and a potential step to 0.5 V was applied. The current response was monitored over a couple of minutes.

The current decays with $t^{1/2}$ at very short times as shown in Figure 9. This behavior is expected by the combined control of electrochemical reaction and diffusion.[21] The values of the current extrapolated to $t = 0$ represent the kinetic process associated to the given CO coverage θ_{CO}. Although the initial adlayer was saturated, diminishing the concentration of CO in the bulk of the solution can change the surface concentration of weakly bonded CO molecules. This affects the kinetic in two aspects: on one side, it changes the desorption energy of CO, and on the other side, it changes the degree of coverage of the species involved in the reaction.

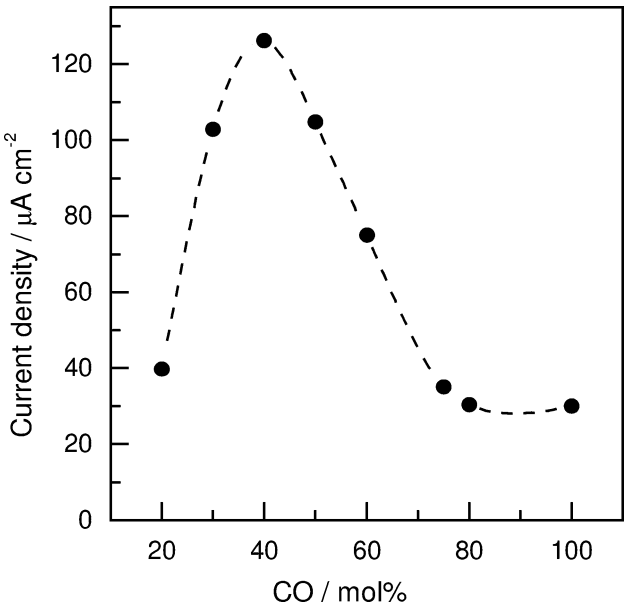

Figure 10. Dependence of the initial current density for CO oxidation at 0.5 V on the composition of the CO/N_2 gas mixture. Pt(111) was 0.1 M $HClO_4$ solution. The values were obtained by extrapolation of the current plots in Figure 9 to $t = 0$.

In Figure 10, the extrapolated values of the current were plotted as a function of the CO concentration in the gas mixture. The results in Figure 10 show that for a concentration of CO of 40% in the gas mixture a maximum rate of oxidation of 126 $\mu A/cm^2$ is attained.

It should be stressed that the degree of coverage by CO during this experiment is almost reaching saturation. Although the relationship between θ_{CO} and bulk CO concentration under these conditions is not known, we assume that increasing the CO partial pressure causes slight changes in θ_{CO}, though keeping the system in the region of low desorption energy.[19]

Saturated CO layers are in equilibrium with CO in the solution, as demonstrated by isotope-exchange experiments.[22] Therefore, although, at the beginning of the experiment, the surface is saturated by bubbling *pure* CO in the solution, some CO molecules desorb during the subsequent step as the CO/N_2 *mixture* replaces the pure gas. Thus, high but slightly different degrees of coverage can be expected for each concentration of CO in the solution. The increasing part of the curve in Figure 10 can be explained as due to the rapid lowering of the energy of desorption with θ_{CO} as the bulk concentration increases. Beyond the maximum, competition with water for adsorption sites to form OH_{ad} hinders the oxidation reaction. This reaction model implies a L−H mechanism for the oxidation of bulk CO.

4. Conclusions

On a Pt(111) electrode in a CO-saturated $HClO_4$ solution, the formation of overlayer structures of CO, previously identified as (2×2)-3CO and $(\sqrt{19} \times \sqrt{19})$-13CO below and above 0.4 V respectively, can be followed by monitoring the bands for 3-fold and 2-fold bonded CO typical of the respective overlayer structure.

When CO is admitted in the cell at 0.05 V, the oxidation of bulk CO occurs at a relatively high rate at potentials below 0.6 V.

The enhanced CO oxidation rate can be rationalized as due to a decrease of the energy of desorption at high degrees of coverage. Because of the equilibrium between weakly adsorbed CO and bulk CO, slight differences in the surface coverage occur

for different partial pressures of CO in the solution, while keeping the total coverage very high. A maximum in the plot of current vs CO bulk concentration is observed under these conditions, which is consistent with a L−H mechanism for the oxidation of bulk CO.

Because of repulsive H_2O−CO interactions, when CO_{ad} is formed at potentials near 0.6 V or higher, water molecules and CO form juxtaposed adlayers. Activation of single H_2O molecules out of the H-bonded H_2O clusters is difficult, and the consequence is an inhibition of bulk CO oxidation.

Acknowledgment. Financial support from FAPESP, CNPq, and CAPES is gratefuly acknowledged. E.A.B. acknowledges a FAPESP fellowship.

References and Notes

(1) Iwasita, T. In *Handbook of Fuel Cells*; Vielstich, W., Lamm, A., Gasteiger, H. A., Eds.; Wiley-UK: Chichester, 2003; Vol. 2, p 603.

(2) Vielstich, W. In *Encyclopedia of Electrochemistry*; Bard, A. J., Stratmann, M., Eds.; Wiley-VCH: Weinheim, 2003; Vol. 2, p 466.

(3) Watanabe, M. In *Handbook of Fuel Cells*; Vielstich, W., Lamm, A., Gasteiger, H. A, Eds.; Wiley-UK: Chichester, 2003; Vol. 2, p 408.

(4) Vielstich, W. *Fuel Cells*; Wiley-Interscience: Bristol, 1965.

(5) Masel, R. I. *Principles of Adsorption and Reaction at Surfaces*; Wiley-Interscience: New York, 1996.

(6) Weaver, M. J.; Zou, S. In *Infrared and Raman Spectroscopy*; Clark, R. J. H., Hester, R. E., Eds.; Wiley: 1998; Vol. 26, Chapter 5.

(7) (a) Kunimatsu, K.; Seki, H.; Gordon, W. G.; Gordon, J. G., II.; Philpot, M. R. *Langmuir* **1986**, *2* (1), 464. (b) Kita, H.; Shimatsu, K.; Kunimatsu, K. *J. Electroanal. Chem.* **1988**, *241*, 163. (c) Marković, N. M.; Lucas, C. A.; Grgur, B. N.; Ross, P. N. *J. Phys. Chem. B* **1999**, *103*, 487. (d) Kita, H.; Narumi, H.; Ye, S.; Naohara, H. *J. Appl. Electrochem.* **1993**, *23*, 589.

(8) (a) Gutiérrez, C.; Caram, A. J. *J. Electroanal. Chem.* **1991**, *305*, 259. (b) Caram, A. J.; Gutiérrez, C. *J. Electroanal. Chem.* **1991**, *308*, 321. (c) Leiva, E. P. M.; Giordano, M. C.; Cervino, R. M.; Arvia, A. J. *J. Electrochem. Soc.* **1986**, *133*, 1660. (d) Kitamura, F.; Taijedo, M.; Takahashi, M.; Ito, M. *Chem. Phys. Lett.* **1986**, *142*, 349. (e) Couto, A.; Pérez, M. C.; Rincón, A.; Gutiérrez, C. *J. Phys. Chem.* **1996**, *100*, 19538.

(9) Wieckowski, A.; Rubel, M.; Gutiérrez, C. *J. Electroanal. Chem.* **1995**, *382*, 97.

(10) Villegas, I.; Weaver, M. J. *J. Chem. Phys.* **1994**, *101*, 1648.

(11) Yoshimi, K.; Song, M.-B.; Ito, M. *Surf. Sci.* **1996**, *368*, 389.

(12) Rodes, A.; Gómez, R.; Feliu, J.; Weaver, M. *Langmuir* **2000**, *16*, 811.

(13) Lucas, C. A.; Markovic, N. m.; Ross, P. N. *Surf. Sci.* **1999**, *425*, L381.

(14) Iwasita, T.; Nart, F. C. In *Progress in Surface Science*; Davison, S. G., Ed.; Pergamon: New York, 1997; Vol. 55, p 271.

(15) Thiel, P. A.; Madey, T. E. *Surf. Sci. Rep.* **1987**, *7*, 211.

(16) *CRC Handbook of Chemistry and Physics*, 80th ed.; Lide, D. R., Ed.; CRC Press: Boca Raton, 1999.

(17) Akemann, W.; Friedrich, K. A.; Stimming, U. *J. Chem. Phys.* **2000**, *113*, 6864.

(18) Kizhakevariam, N.; Jiang, X.; Weaver, M. J. *J. Chem. Phys.* **1994**, *100*, 6575.

(19) Ertl, G.; Newmann, M.; Streit, K. M. *Surf. Sci.* **1977**, *64*, 101.

(20) Koper, M. T. M.; Jansen, A. P. J.; van Santen, R. A.; Lukkiens, J. J.; Hibers, P. A. J. *J. Chem. Phys.* **1998**, *109*, 5061.

(21) Vielstich, W.; Gerischer, H. *Z. Phys. Chem.* **1955**, *4*, 10.

(22) Vogel, U.; Iwasita, T. *Electrochim. Acta* **1988**, *33*, 577.